Journal of Fluids and Structures 17 (2003) 511–523

JOURNAL OF FLUIDS AND STRUCTURES

www.elsevier.nl/locate/jnlabr/yjfls

Flow tones in a pipeline-cavity system: effect of pipe asymmetry

D. Erdem[a], D. Rockwell[a,*], P. Oshkai[a], M. Pollack[b]

[a] *354 Packard Laboratory, Department of Mechanical Engineering, and Mechanics, Lehigh University, 19 Memorial Drive West, Bethlehem, PA 18015, USA*

[b] *Lockheed- Martin, USA*

Received 15 May 2002; received in revised form 11 October 2002

Abstract

Flow tones in a pipeline-cavity system are characterized in terms of unsteady pressure within the cavity and along the pipe. The reference case corresponds to equal lengths of pipe connected to the inlet and outlet ends of the cavity. Varying degrees of asymmetry of this pipe arrangement are investigated. The asymmetry is achieved by an extension of variable length, which is added to the pipe at the cavity outlet. An extension length as small as a few percent of the acoustic wavelength of the resonant mode can yield a substantial reduction in the pressure amplitude of the flow tone. This amplitude decrease occurs in a similar fashion within both the cavity and the pipe resonator, which indicates that it is a global phenomenon. Furthermore, the decrease of pressure amplitude is closely correlated with a decrease of the Q (quality)-factor of the predominant spectral component of pressure. At a sufficiently large value of extension length, however, the overall form of the pressure spectrum recovers to the form that exists at zero length of the extension.

Further insight is provided by variation of the inflow velocity at selected values of extension length. Irrespective of its value, both the magnitude and frequency of the peak pressure exhibit a sequence of resonant-like states. Moreover, the maximum attainable magnitude of the peak pressure decreases with increasing extension length.

1. Introduction

Flow through a pipeline-cavity system represents a generic configuration occurring in a wide variety of applications. Due to the separation of flow along the cavity, the potential exists for coupling between the inherent instability mode of the cavity shear layer and an acoustic mode of the pipeline-cavity system. Even when the inflow to the cavity is fully turbulent, and the acoustic wavelength is much longer than the cavity length, pronounced flow tones can occur (Rockwell et al., 2001). In their investigation, the pipes on either side of the cavity were of the same length and oscillations tended to occur only for the even acoustic modes of the pipeline-cavity system.

Flow tones in a pipeline-cavity system are expected to have certain features in common with tones generated by jet excitation of a long organ pipe (Cremer and Ising, 1967; Fletcher, 1979), jet flow through sequential orifice plates (Wilson et al., 1971; Flatau and Van Moorham, 1990; Hourigan et al., 1990), the wake from a flat plate in a test section (Parker, 1966; Cumpsty and Whitehead, 1971; Stoneman et al., 1988), a shear layer past a cavity resonator (DeMetz and Farabee, 1977; Elder, 1978; Elder et al., 1982; Nelson et al., 1981, 1983), and a cavity shear layer adjacent to a side branch duct/pipe (Pollack, 1980; Bruggeman et al., 1989, 1991; Ziada and Bühlmann, 1992; Kriesels et al., 1995; and

*Corresponding author. Tel.: +1-610-758-4107; fax: +1-610-758-4041.
E-mail address: dor0@lehigh.edu (D. Rockwell).

0889-9746/03/$ - see front matter
doi:10.1016/S0889-9746(02)00159-7

Ziada and Shine, 1999). Selected features of these extensive investigations over the past three decades are briefly summarized by Rockwell et al. (2001).

Directly pertinent to the present work are the tones arising in a pipeline-cavity system, which includes the case where the pipe actually protrudes into the cavity. These investigations were carried out at the University of Southampton and are described in a series of investigations, which extend from Davies (1981) to Davies (1996a, b). Pressure spectra showed a number of pronounced peaks, which indicated the generation of flow tones. For the case of a long pipe terminated by an axisymmetric cavity, Rockwell and Schachenmann (1982, 1983) employed linearized, inviscid stability theory to determine the phase shifts and amplitude spikes across the shear layer and, in addition, characterized the overall phase difference through the cavity during the generation of locked-on flow tones. Rockwell and Karadogan (1982) employed zero-crossing statistics, along with recursive digital filtering, to determine the degree of phase fluctuation of the organized oscillations of turbulent flow through the cavity.

For the configuration of the pipeline-cavity arrangement, which was investigated by Rockwell et al. (2001), the effect of asymmetry, i.e., different lengths of the pipes attached to the inlet and outlet of the cavity, has not been addressed. The following issues therefore remain unclarified:

(i) For the symmetrical pipeline-cavity system, flow tones occur only for even numbered acoustic modes of the pipeline-cavity resonator. This observation suggests that the occurrence of a pressure node, i.e., a velocity antinode, at the location of the cavity is an essential condition for the generation of a locked-on flow tone. A small asymmetry of the pipe arrangement, which corresponds to different lengths of the pipes at the inlet and outlet of the cavity, may effectively detune the locked-on flow tone by shifting the location of the pressure node. The possibility of a substantial reduction in pressure amplitude with a small extension of, for example, the outlet pipe has not been addressed.

(ii) If a substantial reduction in the pressure amplitude can be attained, the issue arises as to whether it occurs for a pipe extension length that is a small fraction of the acoustic wavelength of the resonant mode.

(iii) The consequence of variation of the inflow velocity at a given length of the pipe extension has remained unexplored. The possibility of generation of a sequence of resonant-like states of the magnitude and frequency of the peak pressure amplitude has not been pursued.

(iv) The occurrence of locked-on flow tones is represented by a sharp peak in the pressure spectrum. The effect of the pipe extension on the shape of this peak, more explicitly its quality (Q)-factor, has not been addressed.

(v) For all of the foregoing variations of the peak pressure amplitude, the degree to which they occur globally, i.e., simultaneously at locations within the cavity and within the pipe resonator, has not been addressed.

2. Experimental system and techniques

Complete details of the experimental system are described by Rockwell et al. (2001). Only the essential features are described herein.

Air was supplied from an air compressor, through air treatment and accumulation facilities, located in a separate room, and isolated from the pipeline-cavity system. An inlet plenum served as a settling chamber at the upstream of the pipeline-cavity system. It was lined with acoustic damping foam and contained a honeycomb arrangement. The main pipeline-cavity arrangement consisted of two 7.87 ft (1 ft = 12 in = 304.8 mm) segments of 1 in inner diameter aluminum pipe. The length of the inlet pipe was selected to ensure that the boundary layer at the leading edge of the cavity was fully developed. One pipe segment was located on the upstream side of the Plexiglas cavity and the other on the downstream side. The pipe asymmetry was achieved by a pipe extension at the exit of the downstream pipe. This extension had an inside diameter of 0.96 in and a wall thickness of 0.02 in. The length of its protrusion from the main pipe was continuously varied from 0 to 24.49 in by using one of the three extension pieces lengths: 4.0, 14.0 and 26.0 in. The cavity subsystem for the present experiments, which is shown in Fig. 1, had an internal diameter of 2 in, thereby providing a dimensionless cavity depth $W^* = W/D = 0.5$. The cavity length L was maintained constant at $L = 2.5$ in, corresponding to a dimensionless value $L^* = L/D = 2.5$.

As indicated in Fig. 1, pressure transducer p_a was located within the pipe upstream of the cavity, and transducers p_b and p_c were positioned within the cavity. High-sensitivity PCB transducers (Model U103A02) were employed. The transducer outputs were connected to a PCB Piezotronic multi-channel signal conditioner, Model 48A. In order to prevent aliasing effects, a low-pass filter was applied to all pressure signals. The signals were then transmitted to a National Instruments board, Model PCI-MI0-16-E-4. This board sampled at a rate of 250 000 samples per second, which is well above the requirements of the present experiment. The acquisition of multiple data was accomplished using a multiplexing technique with a scan interval of approximately 32 ms. A Pentium II 350 MHz computer and

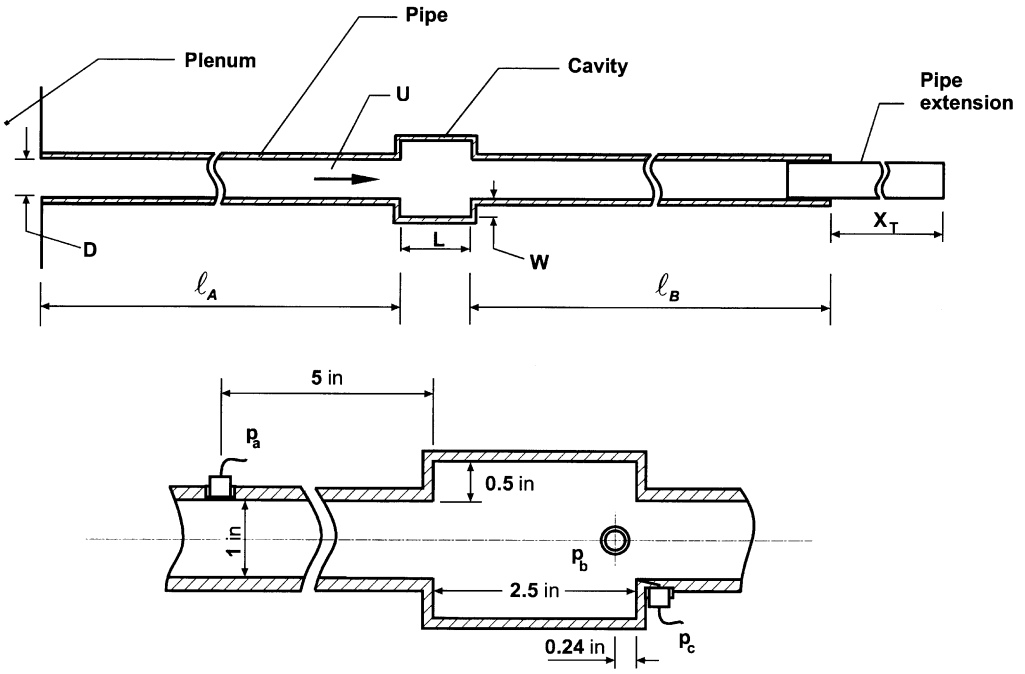

Fig. 1. Overview of pipe-cavity system and locations of pressure transducers.

LabView software were used for processing the transducer signals. During acquisition of data, the sampling rate was set to 4096 samples per second, which resulted in a Nyquist frequency of 2048 Hz. Each of the spectra shown here was obtained by averaging a total of 42 data sets.

3. Effect of variations of length of pipe extension

The three-dimensional plots of Fig. 2 show the magnitude of the pressure peak on a plane of frequency f versus dimensionless pipe extension length X_T/λ. The acoustic wavelength λ is employed as a normalization length. This wavelength is $\lambda = c/f$, in which c is the speed of sound and f is the frequency of the locked-on flow tone for the case $X_T = 0$. The speed of sound corresponding to 21°C and 70% relative humidity is $c = 1,131.53$ ft/s. Therefore, the value of λ at the reference frequency of $f = 620$ Hz was found to be 1.80 ft. Each of the three-dimensional plots corresponds to a different location of the pressure transducer. As defined in Fig. 1, pressure p_a is measured in the pipe resonator at a location upstream of the cavity, pressure p_b on the floor of the cavity, and p_c at the impingement corner of the cavity. The data presented in Figs. 2–6 correspond to the constant inflow velocity of 130 ft/s.

Each of the plots of Fig. 2 shows that the initial increase of X_T/λ produces a decrease in the pressure amplitude p, then at a sufficiently large value of X_T/λ, the amplitude p again increases. At approximately $X_T/\lambda = 0.5$, the amplitude p nearly recovers to its original value at $X_T/\lambda = 0$. The scale of the pressure amplitude p_a is a factor of 5 smaller than the scales on the plots of p_b and p_c, in order to illustrate the similarity in the form of the pressure amplitude response at different locations. The general form of the response is the same at all locations, which indicates that the phenomenon is global. That is, the oscillations of the shear layer along the cavity and the acoustic resonance of the pipeline-cavity system are globally coupled, and attenuation of the pressure amplitude p at one location is necessarily linked to attenuation at other locations as well.

Plan views of the two-dimensional plots are given in Fig. 3. All of these views have a generally similar form. The nominal frequency of interest is the predominant resonant mode at approximately 630 Hz. As the value of X_T/λ increases from zero, the pressure amplitude decreases and, correspondingly, the frequency decreases slightly as well. At approximately $X_T/\lambda = 0.25$, the magnitude of p reaches its lowest value, which is evident in both the lower and upper branches of the shaded pattern. Further increases of X_T/λ yield an increase in pressure amplitude p along the upper branch until a peak value is again attained at approximately $X_T/\lambda = 0.5$. In fact, this same pattern of pressure

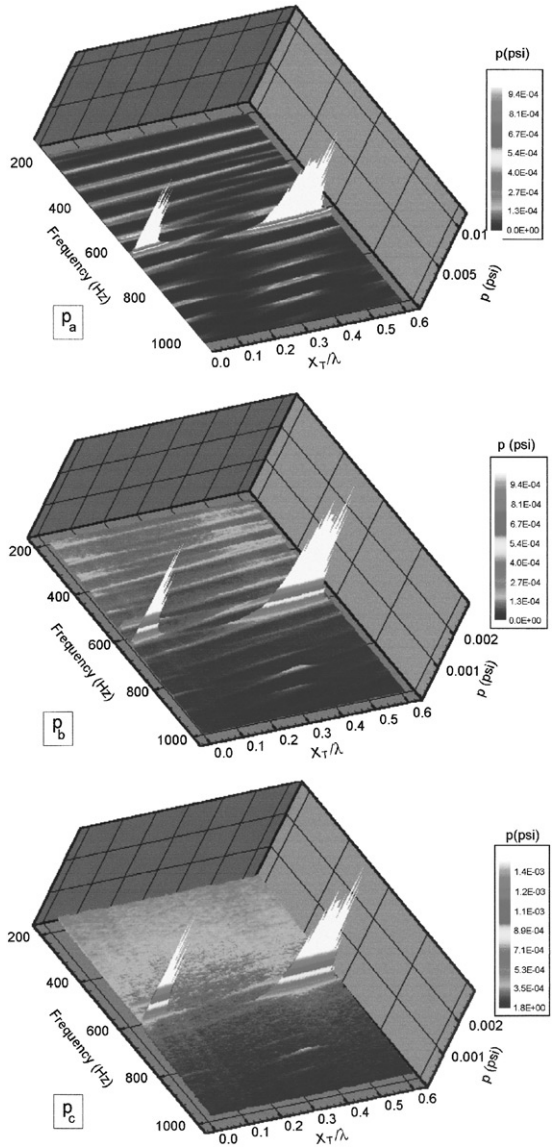

Fig. 2. Three-dimensional representations of pressure amplitude p on a plane of frequency f versus dimensionless pipe extension XT/λ. Plots are shown for the three locations of the pressure transducers defined in Fig. 1.

amplitude p occurs for the resonant modes located below and above the mode of interest, which is nominally at 630 Hz. These modes have significantly lower values of pressure amplitude.

The plots of Fig. 4 show the frequency f_P, the magnitude P of the peak pressure (normalized by its maximum value $P_{\max}$), and Q (quality)-factor of the pressure peak as a function of length X_T of the pipe extension, which is normalized by the pipe diameter D and the acoustic wavelength λ. These distributions correspond to pressure transducer p_a. They were constructed from the data exhibited in the top plots of Figs. 2 and 3.

The variation of f_P in Fig. 4 shows a maximum decrease of 4% at $X_T/\lambda = 0.25$. This decrease is evident along the lower branch of pressure p_a shown in Fig. 3. It compares with a 6.5% decrease predicted from the simple theoretical relationship $f_n = nc/2L_T$, in which L_T is the total length of the pipeline-cavity resonator with the extension X_T. For $X_T/\lambda > 0.25$, the upper branch of p_a in Fig. 3 is considered. The value of f_P in this region is higher than the nominal frequency $f_P = 630$ Hz of the predominant resonant mode. The value of 630 Hz is approached, however, at approximately $X_T/\lambda = 0.5$.

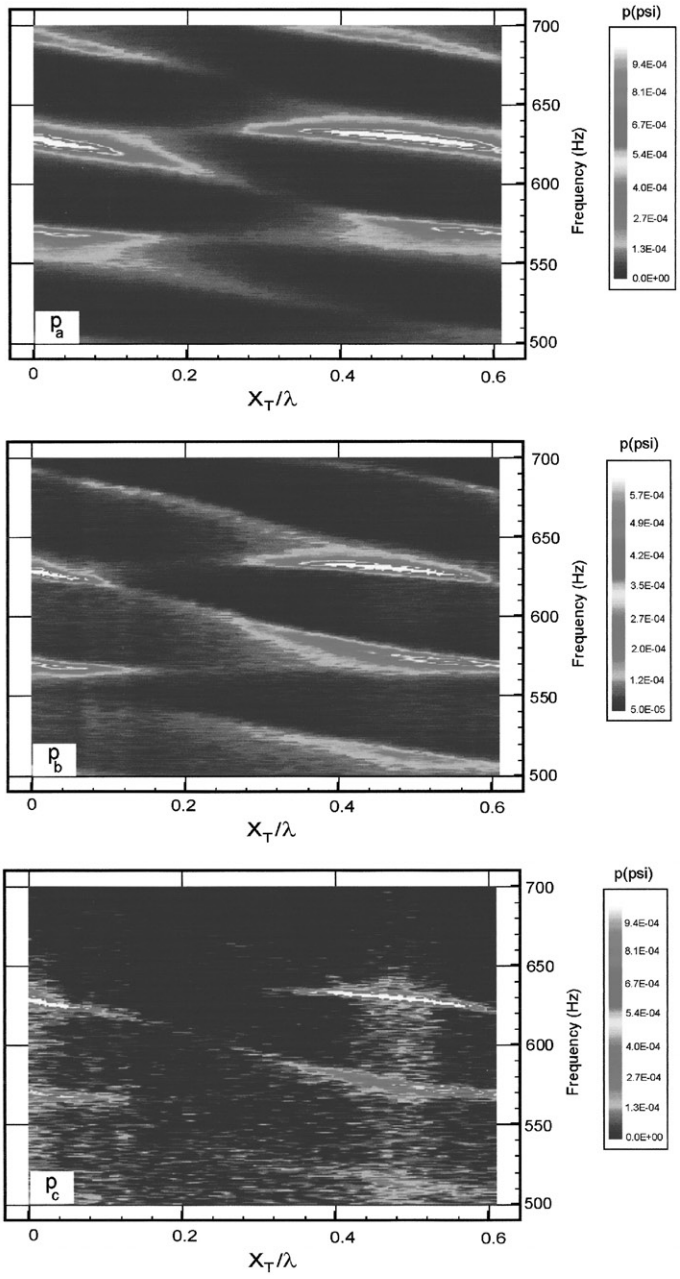

Fig. 3. Plan views of three-dimensional plots of Fig. 2. These views focus on the band of frequencies associated with generation of pronounced peaks of pressure amplitude p.

The corresponding variation of the pressure magnitude $P/P_{\max}$ given in the middle plot of Fig. 4, where $P_{\max}$ refers to the maximum value of pressure P observed for the indicated range of X_T/D, shows a decrease of two orders of magnitude at $X_T/\lambda \approx 0.25$. A substantial decrease of $P/P_{\max}$ is attainable, however, at a small value of X_T/λ. For example, $P/P_{\max}$ decreases to approximately one-third its initial value at approximately $X_T/\lambda = 0.05$, which corresponds to $X_T/D = 1.25$ and $X_T/L = 0.5$, in which L is the cavity length and D is the pipe diameter. On the other hand, at $X_T/\lambda \approx 0.5$, the value of $P/P_{\max}$ recovers to a value close to the value at $X_T/\lambda = 0$. A value of $X_T/\lambda = 0.5$ corresponds to an extension of the standing wave pattern by one-half wavelength and recovery of the value of $P/P_{\max}$.

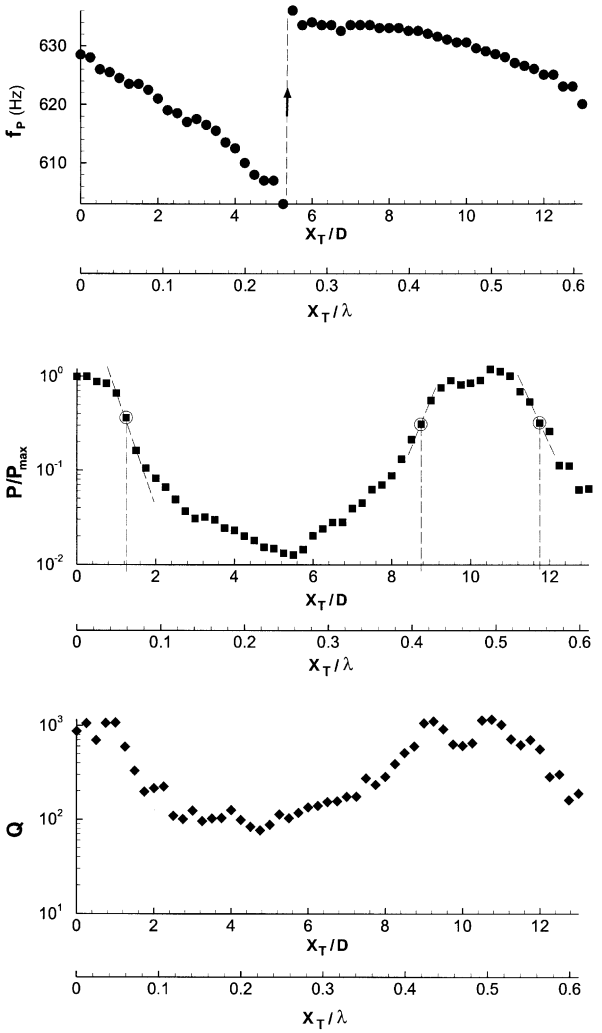

Fig 4. Variations of frequency f_P and magnitude P of predominant pressure peak as a function of length X_T of pipe extension normalized by the pipe diameter D and the acoustic wavelength λ. Also shown is the corresponding variation of the quality (Q)-factor of the corresponding peaks in the pressure spectrum.

The corresponding variation of the quality factor Q, which is exhibited in the bottom plot of Fig. 4, indicates that changes of $P/P_{\max}$ are directly linked to changes in Q. The plot of Q indicates the occurrence of a locked-on flow tone at a zero value of extension, i.e., $X_T/D = X_T/\lambda = 0$, in accord with the findings of Rockwell et al. (2001). In that investigation, values of $Q = 10^3$ corresponded to occurrence of a locked-on flow tone. This value is approximately one order of magnitude larger than the minimum value of Q in the plot of Fig. 4. In fact, the minimum values of $Q \approx 80$–100 are in the general range of the Q-factor of the pipeline-cavity system in absence of throughflow, as determined by transient decay from abrupt termination of loudspeaker excitation and steady-state response to broadband loudspeaker excitation. These experiments were performed during a preliminary phase of this research program. This observation suggests that locked-on flow tones do not exist at, and in the vicinity of, $X_T/\lambda = 0.25$.

Actual spectra are shown for selected values of X_T/D in Fig 5. It should be noted that plots of pressure amplitude versus frequency are referred to as spectra throughout this article. The relation between the values of X_T/λ and X_T/D can be obtained by comparison of the horizontal axes of the plots of Fig. 4. At a sufficiently large value of $X_T/D = 1.5$, the peak amplitude of the predominant spectral component becomes substantially smaller and, at $X_T/D = 2.25$, decreases further. Moreover, the peak values of the side modes also decrease. This observation suggests that the effect of the pipe extension X_T is to attenuate both the predominant locked-on mode and the neighboring modes that are

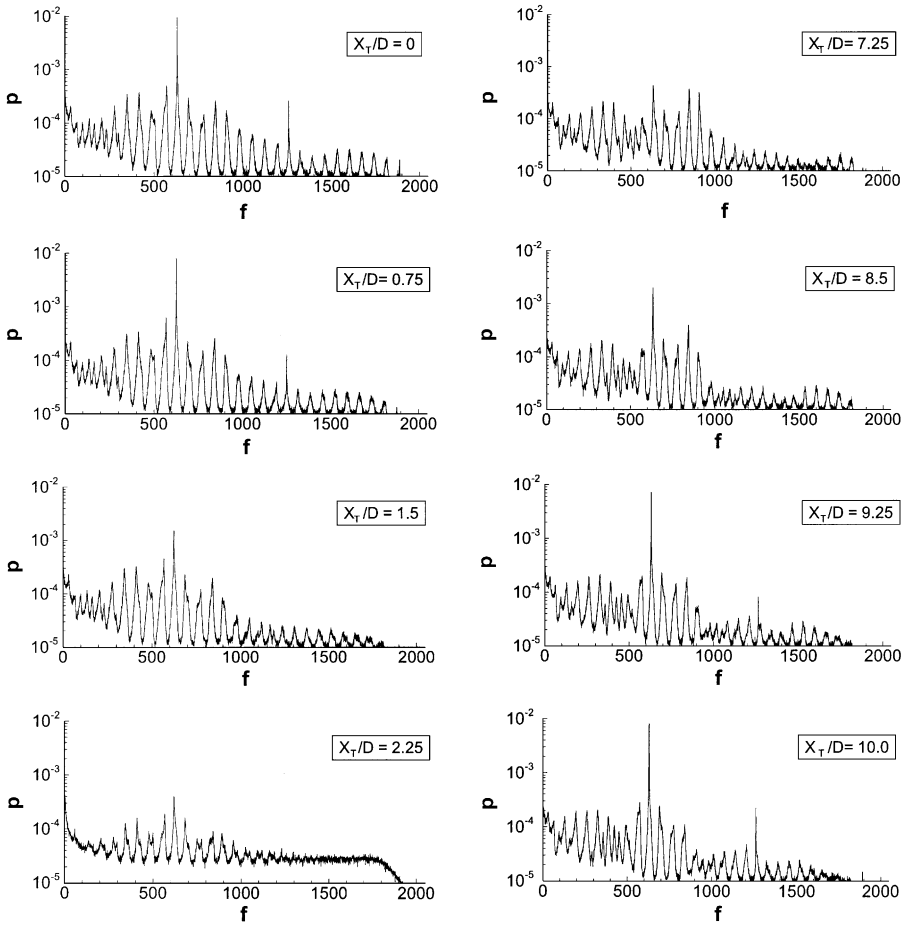

Fig. 5. Selected spectra of the pressure p as a function of length X_T of the pipe extension normalized by the pipe diameter D.

excited by: turbulence within the pipes; and turbulence/instabilities along the shear layer of the cavity. The spectra given in the right column of Fig. 5 show the recovery of the spectral distribution of pressure to approximately its original form for the case of no pipe extension. This recovery is evident from comparison of the spectral distributions at $X_T/D = 0$, 9.25 and 10. Portions of the spectra at $X_T/D = 9.25$ and 10, particularly in the vicinity of 450 and 1000 Hz, do not, however, exhibit the same form as the spectrum at $X_T/D = 0$. Otherwise, the form of the recovered spectrum is quite similar, including occurrence of the first harmonic at approximately 1250 Hz.

Fig. 6 emphasizes the variation in shape of the predominant spectral component of each of the spectra of Fig. 5. For purposes of comparison, the scale on the vertical ordinate of each plot of Fig. 6 is adjusted to produce approximately the same peak amplitude. The increase in width of the spectral peak, which corresponds to a decrease in the value of the Q (quality)-factor, is evident as X_T/D increases from 0 to 2.25. Conversely, decreases in the width of the peak over the range $X_T/D = 7.25$ to 9.25 correspond to increases of the value of Q. At $X_T/D = 10.0$, the width of the spectral peak again decreases, due largely to the uncertainty of the Q-factor calculation, which is highly sensitive to the frequency resolution. Nevertheless, the value of Q remains sufficiently high that the tone remains locked on. That is, Q is well above the aforementioned maximum values of $Q \approx 80$–100.

4. Effect of variations of inflow velocity at constant value of pipe extension length

The data described in the foregoing section show the substantial changes in frequency f_P, peak amplitude $P/P_{\max}$ and quality factor Q with changes in length of the pipe extension X_T at a given value of inflow velocity U. In this section, emphasis is on the variation of the inflow velocity U at selected values of the extension length X_T.

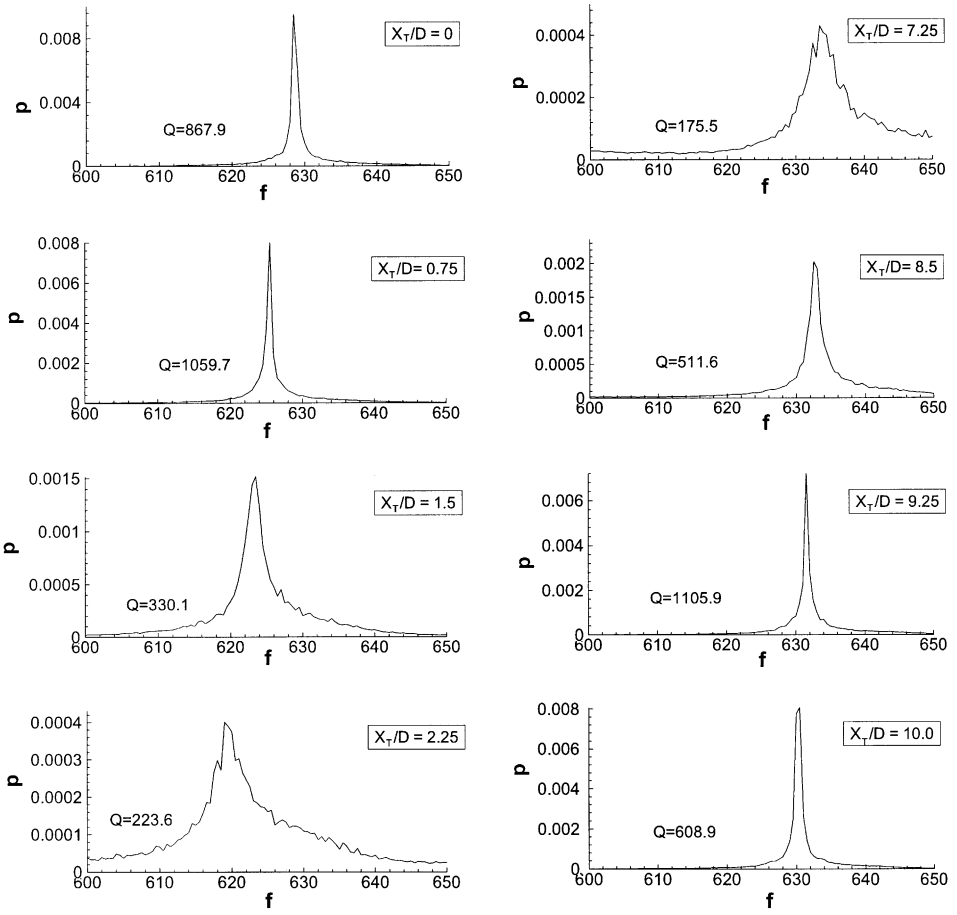

Fig. 6. Zoomed-in plots of the predominant spectral peaks of Fig. 5. Note that the amplitude scale of pressure p is adjusted to give approximately the same height in each plot, thereby providing an aid to interpreting the quality (Q)-factor of the spectral peak.

The three-dimensional plots of Fig. 7 correspond to values of $X_T/D = 0.25$ and 1.5. Note that the vertical scale of the plot at $X_T/D = 0.25$, which represents the amplitude of the pressure p, has been compressed by a factor of four relative to the vertical scale at $X_T/D = 1.5$. This compression allows direct comparison of the general form of the plots at $X_T/D = 0.25$ and 1.5. It is evident that the overall response of the pressure amplitude p and the frequency f_P with variation of the inflow velocity U is generally similar for both cases, despite the substantially lower magnitudes of p at $X_T/D = 1.5$. In essence, both plots show a similar, stage-like behavior. That is, the oscillation jumps to successively higher resonant modes of the pipeline-cavity system as velocity U increases. Moreover, within each resonant mode, a relatively large value of pressure p is attained; near the jump from one mode to the next, the value of pressure p becomes relatively small.

These features are shown more explicitly in the plots of Fig. 8, which exhibit the peak pressure amplitude P and the corresponding frequency f_p taken from the spectrum at each value of U. At values of $X_T/D = 0.25$, 1.0 and 1.5, the values of P occur at approximately the center of each of the resonant modes of the plot of f_P, which is exhibited in the right column. In fact, this general tendency is discernible at the largest value of $X_T/D = 2$, even though this is not a case of true lock-on, as is evident from the low values of $P/P_{\max}$ and Q shown in the plots of Fig. 4.

Fig. 9 shows the data of Fig. 8 superposed on common axes of P versus U and f_P versus U. The legend that defines the symbols for values of X_T/D is valid for both plots. In the top plot, two sets of symbols are filled, in order to allow better distinction between variations of P versus U. The maximum values of P shift to lower values of inflow velocity U as X_T/D increases from 0.25 to 1.0. Further increases of X_T/D result in either an increase, or an indiscernible change, of the velocity U at which peaks of P occur. Regarding the frequency f_P, the value of X_T/D has a detectable effect on the value of U at which the frequency jumps to the next mode. It varies over the range $131 \leqslant U \leqslant 134$ ft/s.

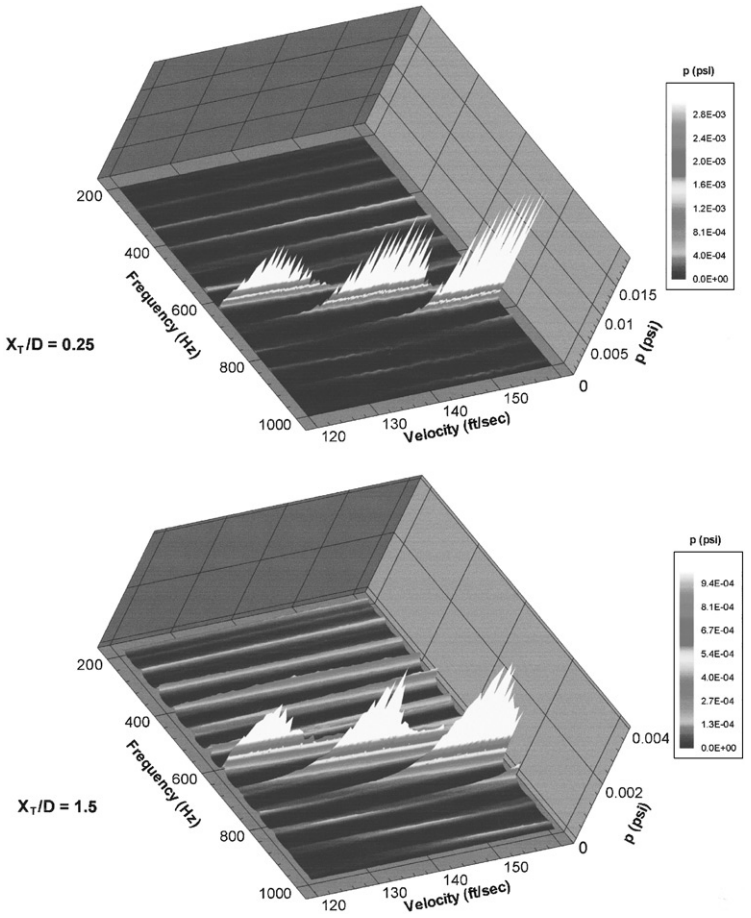

Fig. 7. Three-dimensional plots of the pressure amplitude p on a plane of frequency f and inflow velocity U for two different values of pipe extension length X_T normalized by pipe diameter D.

Selected spectra of pressure p, which correspond to the data sets of Figs. 8 and 9, are given in Fig. 10. For each spectrum, the values of X_T/D and U are indicated. The criterion for selection of the value of U is as follows. It corresponds to the first peak in each distribution of amplitude P in Fig. 8. The general form of the spectra of Fig. 10 is quite similar. At the largest value of $X_T/D = 2.0$, attenuation of the peak at the predominant component of 680 Hz is accompanied by disappearance of the distinctive first harmonic at 1360 Hz.

Zoomed-in plots of the predominant spectral peaks of Fig. 10 are exhibited in Fig. 11. Note that the vertical ordinate of each plot has been adjusted to provide the same peak amplitude, thereby providing a physical portrayal of the decrease in Q-factor with increasing X_T/D. As in Fig. 10, each of these zoomed-in plots is taken at the value of velocity U corresponding to the maximum value of the peak pressure amplitude P. This observation indicates that, irrespective of the variation of velocity U over a relatively wide range in Figs. 7–9, the maximum value of the Q-factor is limited by the value of X_T/D. That is, at successively larger values of X_T/D, the maximum attainable value of Q decreases.

5. Concluding remarks

Flow through a pipeline-cavity system, where the length of the pipe at the cavity inlet is equal to the length at the outlet, is known to give rise to locked-on flow tones. The present investigation has examined the consequences of a difference in length of the inlet and outlet pipes; this was accomplished using an extension of length X_T/D of the outlet pipe. The effects of this extension are summarized below.

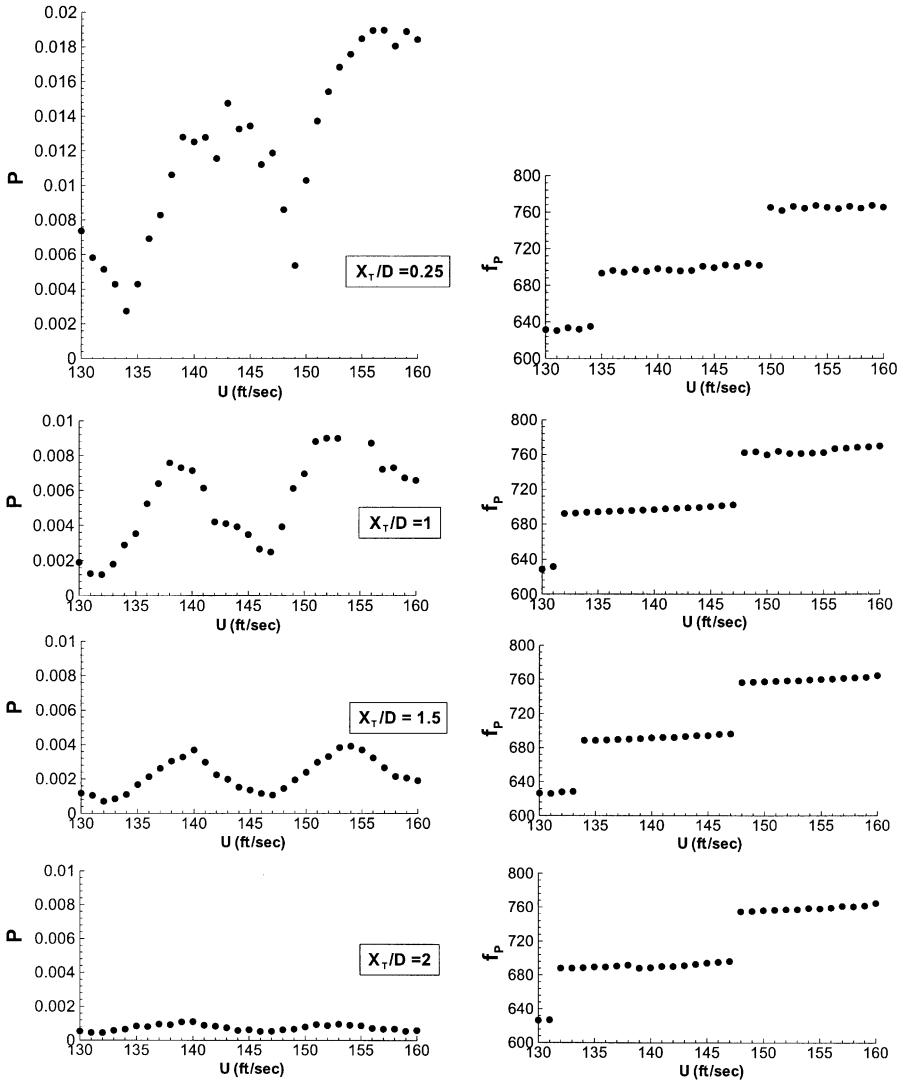

Fig. 8. Variation of peak pressure amplitude P and frequency of peak f_P with inflow velocity U for selected values of pipe extension length X_T normalized by pipe diameter D.

(i) Substantial attenuation of the peak pressure amplitude of a locked-on flow tone occurs when the pipe extension X_T is of the order of a few percent, e.g., 5%, of the acoustic wavelength, $X_T/\lambda = 0.05$. This extension corresponds, however, to approximately one-half the cavity length L, i.e., $X_T/L \approx 0.5$.

(ii) A reduction in the peak pressure amplitude P is associated with a corresponding decrease of the quality factor Q of the predominant pressure peak, as well as a decrease in the frequency f_P of the spectral component corresponding to the peak pressure. In fact, at sufficiently large values of X_T/λ, the values of Q are approximately equal to the values obtained for turbulent flow through a pipe in absence of a cavity. This observation indicates that even a marginally locked-on state does not exist in this range.

(iii) At a sufficiently large value of the pipe extension, corresponding to $X_T/\lambda \approx 0.5$, the amplitude of the peak pressure P, its frequency f_P, and the quality factor Q approximately recover to the values obtained for no pipe extension, $X_T/D = 0$. Moreover, the overall form of the pressure spectrum is generally similar at $X_T/\lambda \approx 0.5$ and 0.

(iv) Variation of the inflow velocity U at a given value of pipe extension X_T/λ yields a sequence of resonant-like states of the peak pressure amplitude. The major features of this sequence of states are successive jumps to higher order modes of the resonant pipeline-cavity system, as well as occurrence of a well-defined maximum of the peak pressure amplitude within each state. This stage-like behavior persists even for larger values of X_T/λ for which the

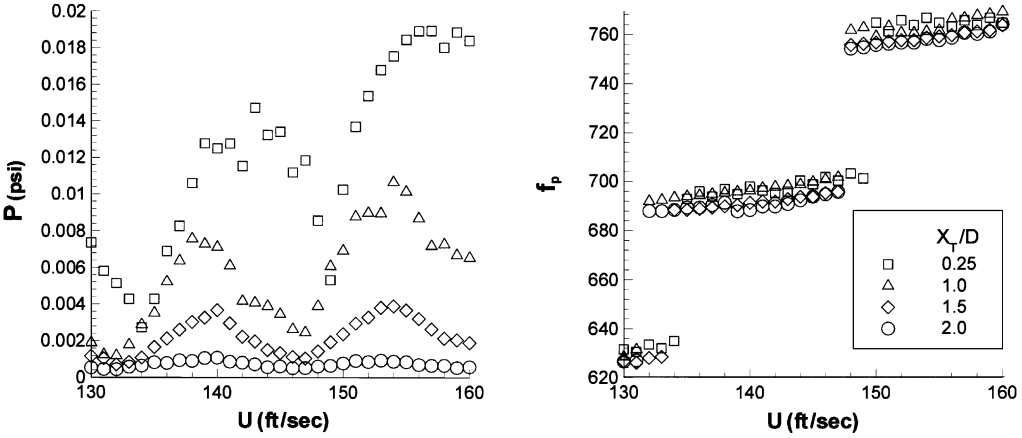

Fig. 9. Variations of Fig. 8 plotted on the same set of axes.

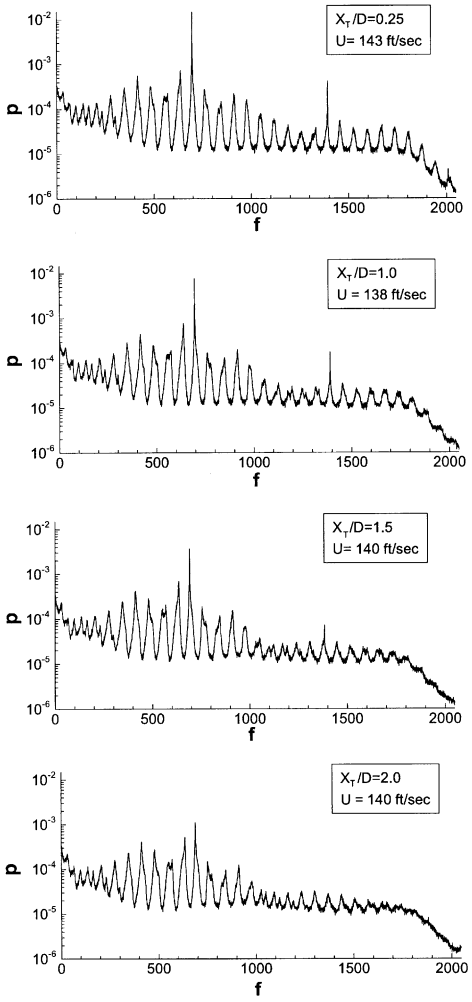

Fig. 10. Selected spectra of pressure p for the data sets of Figs. 8 and 9. The value of velocity U indicated on each plot corresponds to occurrence of the maximum value of peak amplitude P as U is varied.

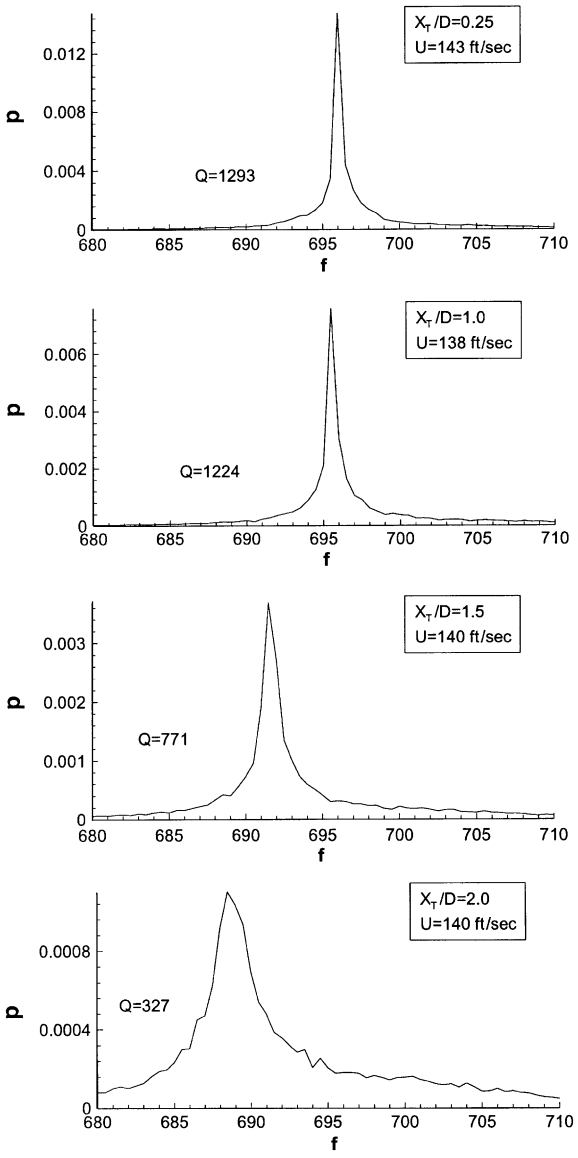

Fig. 11. Zoomed-in plots of spectral peaks corresponding to peak pressure amplitude P in the spectra of Fig. 10.

peak pressure amplitude is substantially attenuated. In essence, the effect of the pipe extension is to limit the value of peak pressure amplitude that can be attained when the inflow velocity U is varied over a substantial range. The overall forms of the pressure amplitude and frequency variations with inflow velocity U are generally similar at different values of X_T/λ.

Acknowledgements

The authors are grateful for financial support under Office of Naval Research Grant No. N00014-98-1-0817.

References

Bruggeman, J.C., Hirschberg, A., van Dongen, M.E.H., Wijnands, A.P.J., Gorter, J., 1989. Flow induced pulsations in gas transport systems: analysis of the influence of closed side branches. ASME Journal of Fluids Engineering 111, 484–491.

Bruggeman, J.C., Hirschberg, A., van Dongen, M.E.H., Wijnands, A.P.J., Gorter, J., 1991. Self-sustained aero-acoustic pulsations in gas transport systems: experimental study of the influence of closed side branches. Journal of Sound and Vibration 150, 371–393.

Cremer, L., Ising, H., 1967/68. Die selbsterregte schwingungen von orgelpfeifen. Acustica 19, 143–153.

Cumpsty, N.S., Whitehead, D.S., 1971. The excitation of acoustic resonances by vortex shedding. Journal of Sound and Vibration 18, 353–369.

Davies, P.O.A.L., 1981. Flow-acoustic coupling in ducts. Journal of Sound and Vibration 77, 191–209.

Davies, P.O.A.L., 1996a. Piston engine intake and exhaust system design. Journal of Sound and Vibration 190, 677–712.

Davies, P.O.A.L., 1996b. Aeroacoustics and time varying systems. Journal of Sound and Vibration 190, 345–362.

Demetz, F.C., Farabee, T.M., 1977. Laminar and turbulent shear flow-induced resonances. AIAA Paper 77–1293.

Elder, S.A., 1978. Self-excited depth-mode resonance for a wall-mounted cavity in turbulent flow. Journal of the Acoustical Society of America 64, 877–890.

Elder, S.A., Farabee, T.M., Demetz, F.C., 1982. Mechanisms of flow-excited cavity tones at low mach number. Journal of the Acoustical Society of America 72, 532–549.

Flatau, A., van Moorham, W.K., 1990. Prediction of vortex shedding responses in segmented solid rocket motors. AIAA Paper 90–2073.

Fletcher, N.H., 1979. Airflow and sound generation in musical wind instruments. Annual Review of Fluid Mechanics 11, 123–146.

Hourigan, K., Welsh, M.C., Thompson, M.C., Stokes, A.N., 1990. Aerodynamic sources of acoustic resonance in a duct with baffles. Journal of Fluids and Structures 4, 345–370.

Kriesels, P.C., Peters, M.C.A.M., Hirschberg, A., Wijnands, A.P.J., Iafrati, A., Riccaradi, G., Piva, R., Bruggemann, J.-C., 1995. High amplitude vortex-induced pulsations in a gas transport system. Journal of Sound and Vibration 184, 343–368.

Nelson, P.A., Halliwell, N.A., Doak, P.E., 1981. Fluid dynamics of a flow excited resonance, Part I: experiment. Journal of Sound and Vibration 78, 15–38.

Nelson, P.A., Halliwell, N., Doak, P.E., 1983. Fluid dynamics of a flow excited resonance, Part II: Flow acoustic interaction. The dissipation of sound at an edge. Journal of Sound and Vibration 91, 375–402.

Parker, R., 1966. Resonance effects in wake shedding from parallel plates: some experimental observations. Journal of Sound and Vibration 4, 62–72.

Pollack, M.L., 1980. Flow-induced tones in side-branch pipe resonators. Journal of the Acoustical Society of America 67, 1153–1156.

Rockwell, D., Karadogan, H., 1982. Oscillations of an impinging turbulent jet: coherence characterization via conditional sampling. Journal of Sound and Vibration 83 (1), 111–124.

Rockwell, D., Schachenmann, A., 1982. Self-generation of organized waves in an impinging turbulent jet at low Mach numbers. Journal of Fluid Mechanics 117, 425–441.

Rockwell, D., Schachenmann, A., 1983. The organized shear layer due to oscillations of a turbulent jet through an axisymmetric cavity. Journal of Sound and Vibration 87, 371–382.

Rockwell, D., Lin, J.-C., Oshkai, P., Reiss, M., Pollack, M., 2001. Shallow cavity flow tone experiments: onset of locked-on states. Journal of Fluids and Structures, submitted for publication.

Stoneman, S.A.T., Hourigan, K., Stokes, A.N., Welsh, M.E., 1988. Resonant sound caused by flow past two plates in tandem in a duct. Journal of Fluid Mechanics 192, 455–484.

Wilson, T.A., Beavers, G.S., Decoster, M.A., Holger, D.K., Regenfuss, M.D., 1971. Experiments on the fluid mechanics of whistling. Journal of the Acoustical Society of America 50, 366–372.

Ziada, S., Bühlmann, E.T., 1992. Self-excited resonances of two-side-branches in close proximity. Journal of Fluids and Structures 6, 583–601.

Ziada, S., Shine, S., 1999. Strouhal numbers of flow-excited acoustic resonance of closed side branches. Journal of Fluids and Structures 13, 127–142.